ARMY RESEARCH LABORATORY

Understanding Body-Fixed Sensor Output From Projectile Flight Experiments

Thomas E. Harkins

ARL-TR-3029 **September 2003**

Approved for public release; distribution is unlimited

NOTICES

Disclaimers

The findings in this report are not to be construed as an official Department of the Army position unless so designated by other authorized documents.

Citation of manufacturers' or trade names does not constitute an official endorsement or approval of the use thereof.

DESTRUCTION NOTICE¾Destroy this report when it is no longer needed. Do not return it to the originator.

Army Research Laboratory
Aberdeen Proving Ground, MD 21005-5066

ARL-TR-3029 September 2003

Understanding Body-Fixed Sensor Output From Projectile Flight Experiments

Thomas E. Harkins
Weapons and Materials Research Directorate

Approved for public release; distribution is unlimited

REPORT DOCUMENTATION PAGE

Form Approved
OMB No. 0704-0188

Public reporting burden for this collection of information is estimated to average 1 hour per response, including the time for reviewing instructions, searching existing data sources, gathering and maintaining the data needed, and completing and reviewing the collection of information. Send comments regarding this burden estimate or any other aspect of this collection of information, including suggestions for reducing the burden, to Department of Defense, Washington Headquarters Services, Directorate for Information Operations and Reports (0704-0188), 1215 Jefferson Davis Highway, Suite 1204, Arlington, VA 22202-4302. Respondents should be aware that notwithstanding any other provision of law, no person shall be subject to any penalty for failing to comply with a collection of information if it does not display a currently valid OMB control number.
PLEASE DO NOT RETURN YOUR FORM TO THE ABOVE ADDRESS.

1. REPORT DATE *(DD-MM-YYYY)*	2. REPORT DATE	3. DATES COVERED (From - To)
September 2003	Final	

4. TITLE AND SUBTITLE

Understanding Body-Fixed Sensor Output From Projectile Flight Experiments

5a. CONTRACT NUMBER

5b. GRANT NUMBER

5c. PROGRAM ELEMENT NUMBER
1L162618

6. AUTHOR(S)

Harkins, T.E. (ARL)

5d. PROJECT NUMBER
H80

5e. TASK NUMBER

5f. WORK UNIT NUMBER

7. PERFORMING ORGANIZATION NAME(S) AND ADDRESS(ES)

U.S. Army Research Laboratory
Weapons and Materials Research Directorate
Aberdeen Proving Ground, MD 21005-5066

8. PERFORMING ORGANIZATION REPORT NUMBER

ARL-TR-3029

9. SPONSORING/MONITORING AGENCY NAME(S) AND ADDRESS(ES)

10. SPONSOR/MONITOR'S ACRONYM(S)

11. SPONSOR/MONITOR'S REPORT NUMBER(S)

12. DISTRIBUTION/AVAILABILITY STATEMENT

Approved for public release; distribution is unlimited.

13. SUPPLEMENTARY NOTES

14. ABSTRACT

Accurate measurement of in-flight kinematics significantly contributes to the development of experimental projectiles and rockets and to diagnostics for existing munitions and weapons systems. Ground-based instruments such as radar and cameras provide useful measurements but are often limited to portions of a trajectory and/or have limited resolution. On-board sensor systems fixed to a projectile body combined with a telemetry system can provide high resolution continuous data throughout a projectile's entire trajectory.

However, there is a twofold difficulty in correctly interpreting and employing data from body-fixed sensors. First, sensor responses many times are affected by stimuli other than those which a sensor is intended to quantify, e.g., an angular rate sensor may be affected by any g forces to which it is subjected. Second, sensor systems often, of necessity, make measurements in a body-fixed coordinate system, and the quantities whose values are desired are best described in another coordinate system. This report treats issues affecting the output of the body-fixed sensors used by the U.S. Army Research Laboratory's Weapons and Materials Research Directorate (Advanced Munitions Concepts Branch) in flight tests of military ordnance and provides the mathematics necessary to transform body-fixed measurements to earth-fixed parameters.

15. SUBJECT TERMS

body-fixed sensors diagnostic fuze projectile kinetics

16. SECURITY CLASSIFICATION OF			17. LIMITATION OF ABSTRACT	18. NUMBER OF PAGES	19a. NAME OF RESPONSIBLE PERSON
a. REPORT	b. ABSTRACT	c. THIS PAGE			Thomas E. Harkins
Unclassified	Unclassified	Unclassified	UL	30	19b. TELEPHONE NUMBER *(Include area code)* 410-306-0850

Standard Form 298 (Rev. 8/98)
Prescribed by ANSI Std. Z39.18

Contents

List of Figures

1. Introduction

Accurate measurement of in-flight kinematics significantly contributes to the development of experimental projectiles and rockets and to diagnostics for existing munitions and weapons systems. Such measurements can in some cases be made with high speed photography, but this technique is generally used for only limited portions of a projectile flight for reasons of expense and practicability. Also, the precision of angular measurements is limited in this methodology. Another measurement technique used for obtaining angle of attack data is yaw cards, but this technique also is low resolution and provides only a small number of discrete data points along a trajectory. Radar can provide position, velocity, and spin measurements but does not give projectile orientation information. Global positioning systems provide position and velocity measurements but cannot provide orientation information. On-board sensor systems fixed to a projectile body combined with a telemetry system can provide continuous measurements throughout a projectile's entire trajectory.

The Advanced Munitions Concepts Branch of the U.S. Army Research Laboratory's (ARL's) Weapons and Materials Research Directorate has for many years designed, built, and employed body-fixed sensor systems in support of military ordnance development and testing. Sometimes, a quantity of interest to a tester is directly measurable, and given an accurate sensor, only the observation or recording of sensor data is required to meet test objectives. Temperature is one example of such a quantity. In other cases, body-fixed sensors' output needs to be combined and/or otherwise processed in order to obtain measures of desired quantities. For example, a post-launch, time history of both speed and heading is required to locate a flying body. Combining/processing is also often required for correct interpretation of output from body-fixed sensors responding to stimuli external to the flight body. Vector magnetometers measuring components of the earth's magnetic field are an example of such sensors.

In essence, there is a twofold difficulty in correctly interpreting and employing data from body-fixed sensors. First, sensor responses many times are affected by stimuli other than those that a sensor is intended to quantify, e.g., an angular rate sensor may be affected by any g forces to which it is subjected. Second, sensor systems often, of necessity, make measurements in a body-fixed coordinate system, and the quantities whose values are desired are best described in another coordinate system. Although coordinate transforms are a staple of high school trigonometry classes, it nevertheless is useful to clearly define the coordinate system conventions and rigorously develop the transformations employed at ARL when we provide instrumentation and data collection/processing support for projectile flight experiments. It is hoped that this elementary and somewhat tedious exposition will benefit interpreters of body-fixed sensor data and other readers by familiarizing them with the issues involved and thereby avoid the confusion that we sometimes have observed with regard to such data.

To this end, three Cartesian systems commonly employed in projectile test and evaluation are defined and the mathematics necessary to transform among them are given in this report. Examples of idealized projectile-fixed sensor output from projectile trajectory simulations and sensor output recorded during flight experiments will illustrate this process. An additional coordinate system extensively employed in computer modeling and simulation of projectile flight is treated in Appendix A.

2. Coordinate Systems

The first coordinate system is convenient for describing the motion of a gun- or tube-launched projectile along its trajectory. This system is right-handed Cartesian with its origin at the launch site. This is referred to as the "earth-fixed" system herein, and parameters in this system are subscripted with an "E". The axes are defined as follows (see Figure 1):

- The X_E and Y_E axes define a plane tangent to the earth's surface at the origin.
- The Z_E axis is perpendicular to the earth's surface with positive downward, i.e., in the direction of gravity.
- The X_E axis is chosen so that the centerline of the launcher is in the X_E-Z_E plane.

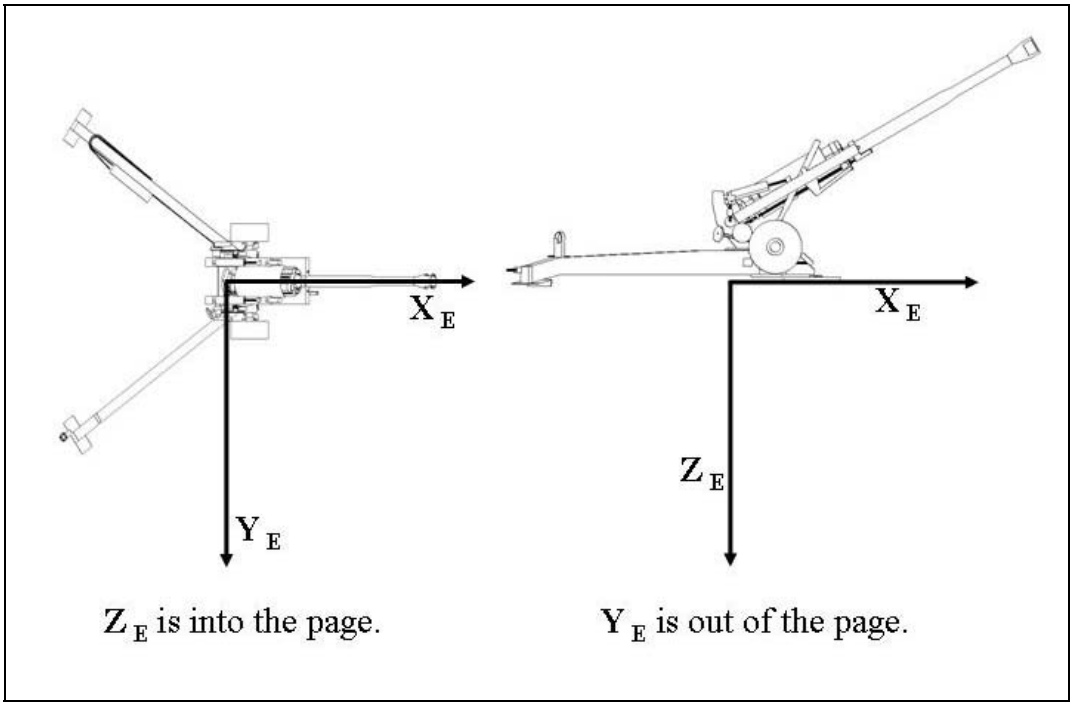

Figure 1. Earth-fixed coordinate system.

Down-range travel is then measured along the X_E axis, deflection is measured along the Y_E axis (positive to the right when one is looking down range), and altitude is measured along the Z_E axis (positive downward). Designation of height above the ground as a negative Z_E component of projectile location may seem unnatural to some, but this coordinate system was employed by a former division chief at ARL, Dr. Charles Murphy, in his seminal work on free-flight motion of symmetric projectiles (Murphy, 1963), and this became the norm within ARL.

The second system is convenient for aeroballistic computations of rigid projectiles' flights and for describing the locations and orientations of such projectiles' components. This system is right-handed Cartesian with its origin at the center of gravity (c.g.) of the flight body (see Figure 2). This is referred to as the "projectile-fixed" system herein, and parameters in this system are subscripted with a "P".

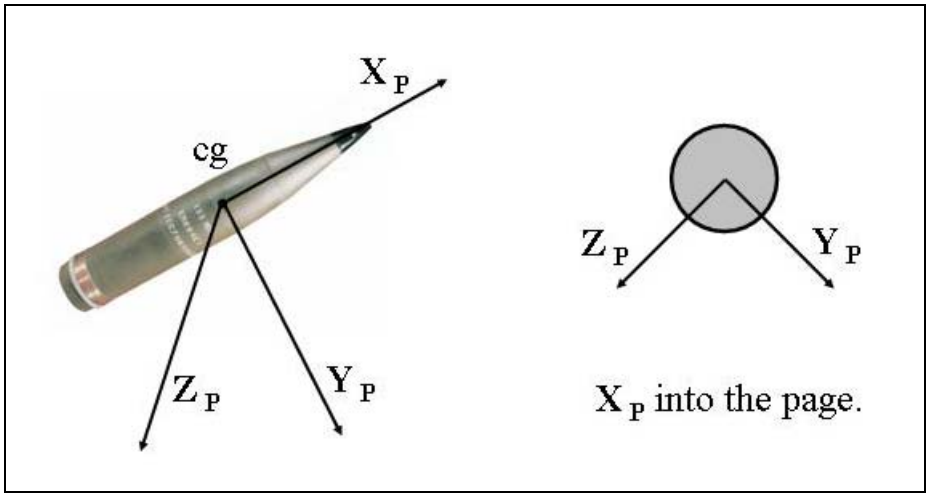

Figure 2. Projectile-fixed coordinate system.

Most of the projectiles instrumented by ARL are either spin-stabilized or are designed to have some fin cant-induced roll rate to mitigate the effects of asymmetries. For such flight bodies, the X_P axis of the projectile-fixed coordinate system usually lies along the projectile axis of symmetry, i.e., the spin axis (with positive in the direction of travel at launch). The Y_P and Z_P axes are then oriented so as to complete the right-handed orthogonal system. Because the Y_P and Z_P axes are collinear with projectile radii in the cross section through the c.g., sensors whose axes are parallel with this cross section are commonly termed "radial" sensors. Similarly, sensors whose axes are parallel with the X_P axis are commonly termed "axial" sensors.

The third coordinate system is commonly employed to specify locations on or near the earth's surface (i.e., north, east, and down). This is referred to as the "navigation" system herein, and parameters in this system are subscripted with an "N". Thus, north = X_N, east = Y_N, and down = Z_N.

3. Transformations With Euler Angles

The specification of a vector in any Cartesian system can be transformed into its corresponding specification in any other Cartesian system in two steps. First, the origins must be made coincident through a translation. The second step is to perform three successive rotations in a specified sequence. The three successive rotation angles are called Euler angles. This relationship is illustrated for the earth-fixed and projectile-fixed systems in Figure 3 where the gray ball's position in the earth-fixed system is given by $\vec{P}_E$ and its position in the projectile-fixed system by $\vec{P}_P$. If the location as measured in the first system of second system's origin at the projectile c.g. is $\vec{O}_E$, then the vector from that origin to the ball, as measured in the first system, is $\vec{L}_E$, which can be obtained from the translation equation $\vec{P}_E = \vec{O}_E + \vec{L}_E$. We can then derive $\vec{P}_P$ from $\vec{L}_E$ by performing the Euler rotations necessary to obtain the orientations of the X_P, Y_P, and Z_P axes.

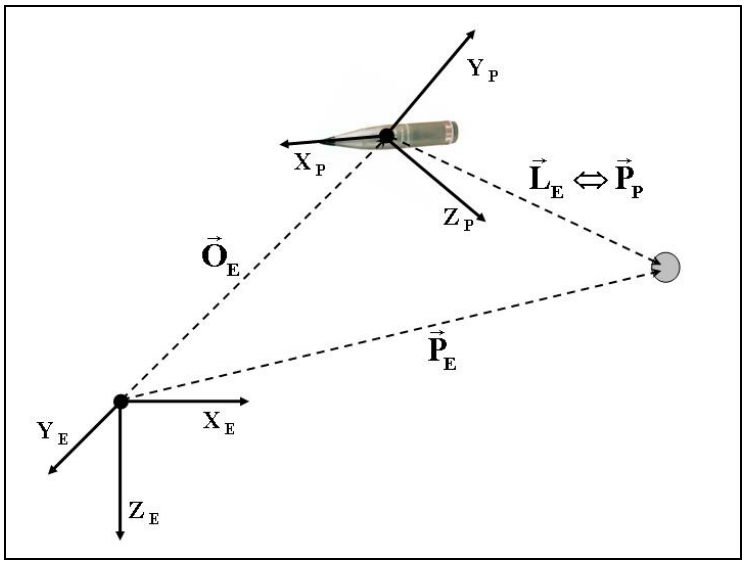

Figure 3. Position of a ball as measured in two coordinate systems.

After the translational offset to collocate the origins of the earth-fixed and projectile-fixed systems has been subtracted, transformations of vectors from the earth-fixed system to the projectile-fixed system via Euler rotations proceed as follows:

1. Rotate the X_E, Y_E, Z_E system about the Z_E axis through an angle ε_1 where ε_1 is measured in the direction of rotation of the head of a right-hand screw advancing along the Z_E axis (see Figure 4). Call the resulting axes X_1, Y_1, Z_1 in which $Z_1 = Z_E$. ε_1 is the angle

between the X_E axis and the projection of the X_P axis into the $X_E \mid Y_E$ plane. Thus, the projectile's spin axis is in the $X_1 \mid Z_1$ plane with its nose in the $+X_1 \mid Z_1$ half-plane.

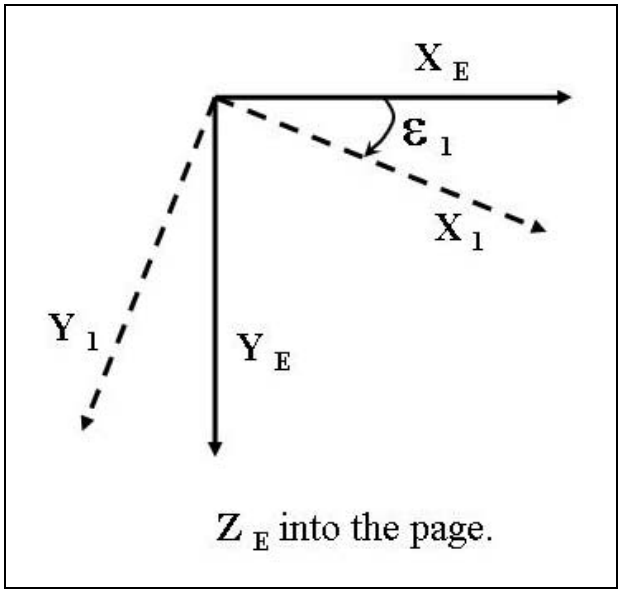

Figure 4. First Euler rotation.

If the coordinates of a vector $\vec{V}$ are denoted by the column matrix $\begin{pmatrix} a_E \\ b_E \\ c_E \end{pmatrix}$ in the earth-fixed system and denoted by $\begin{pmatrix} a_1 \\ b_1 \\ c_1 \end{pmatrix}$ in the X_1, Y_1, Z_1 system, then the coordinates are related by the equations

$$\begin{aligned} a_1 &= a_E \cos(\varepsilon_1) + b_E \sin(\varepsilon_1) \\ b_1 &= -a_E \sin(\varepsilon_1) + b_E \cos(\varepsilon_1) \\ c_1 &= c_E \end{aligned} \tag{1}$$

or, in matrix form,

$$\vec{V}_1 = E_1 \vec{V}_E \tag{2}$$

in which

$$E_1 = \begin{pmatrix} \cos(\varepsilon_1) & \sin(\varepsilon_1) & 0 \\ -\sin(\varepsilon_1) & \cos(\varepsilon_1) & 0 \\ 0 & 0 & 1 \end{pmatrix} \tag{3}$$

2. Rotate the X_1, Y_1, Z_1 system about the Y_1 axis through an angle ε_2 measured in the direction of rotation of the head of a right-hand screw advancing along the Y_1 axis (see Figure 5). Call the resulting axes X_2, Y_2, Z_2 in which $Y_2 = Y_1$. ε_2 is the angle between the

projectile spin axis and the X_1 axis so that the projectile spin axis lies along the X_2 axis. In other words, $X_2 = X_P$.

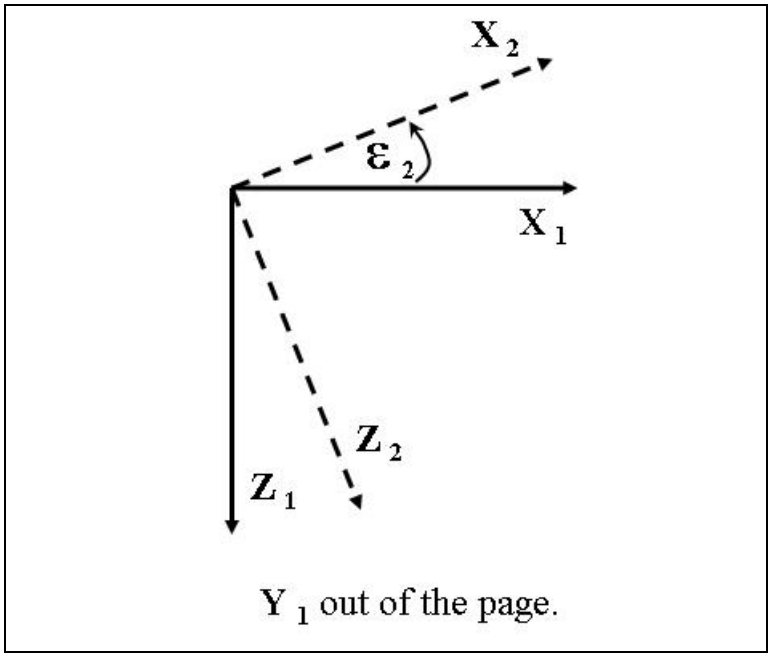

Figure 5. Second Euler rotation.

If the coordinates of $\vec{V}$ are denoted by $\begin{pmatrix} a_2 \\ b_2 \\ c_2 \end{pmatrix}$ in the X_2, Y_2, Z_2 system, then the coordinates are related by the equations

$$\begin{aligned} a_2 &= a_1 \cos(\varepsilon_2) - c_1 \sin(\varepsilon_2) \\ b_2 &= b_1 \\ c_2 &= a_1 \sin(\varepsilon_2) + c_1 \cos(\varepsilon_2) \end{aligned} \tag{4}$$

or, in matrix form,

$$\vec{V}_2 = E_2 \vec{V}_1 = E_2 E_1 \vec{V}_E \tag{5}$$

in which

$$E_2 = \begin{pmatrix} \cos(\varepsilon_2) & 0 & -\sin(\varepsilon_2) \\ 0 & 1 & 0 \\ \sin(\varepsilon_2) & 0 & \cos(\varepsilon_2) \end{pmatrix} \tag{6}$$

3. Rotate the X_2, Y_2, Z_2 system about the X_2 axis through an angle ε_3 measured in the direction of rotation of the head of a right-hand screw advancing along the X_2 axis (see Figure 6). Call the resulting axes X_3, Y_3, Z_3 in which $X_3 = X_2 = X_P$. ε_3 is chosen so that $Y_3 = Y_P$ and consequently, $Z_3 = Z_P$.

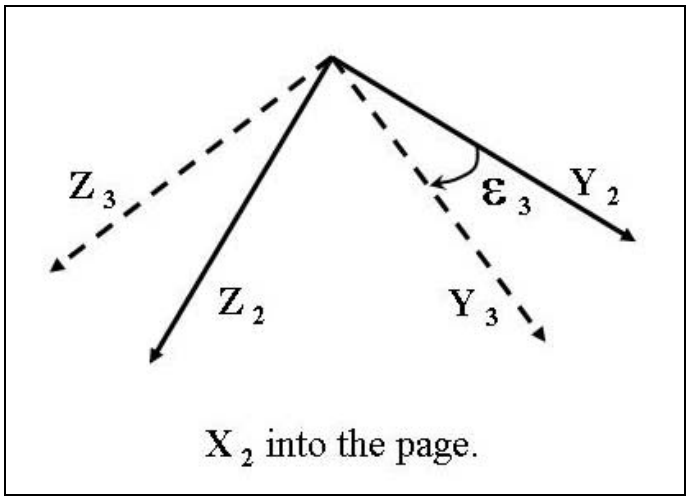

Figure 6. Third Euler rotation.

If the coordinates of $\vec{V}$ are denoted by $\begin{pmatrix} a_3 \\ b_3 \\ c_3 \end{pmatrix}$ in the X_3, Y_3, Z_3 system, then the coordinates are related by the equations

$$\begin{aligned} a_3 &= a_2 \\ b_3 &= b_2 \cos(\varepsilon_3) + c_2 \sin(\varepsilon_3) \\ c_3 &= -b_2 \sin(\varepsilon_3) + c_2 \cos(\varepsilon_3) \end{aligned} \tag{7}$$

or, in matrix form,

$$\vec{V}_3 = E_3 \vec{V}_2 = E_3 E_2 E_1 \vec{V}_E \tag{8}$$

in which

$$E_3 = \begin{pmatrix} 0 & 0 & 1 \\ 0 & \cos(\varepsilon_3) & \sin(\varepsilon_3) \\ 0 & -\sin(\varepsilon_3) & \cos(\varepsilon_3) \end{pmatrix} \tag{9}$$

Recognizing that the X_3, Y_3, Z_3 system is the same as the projectile-fixed X_P, Y_P, Z_P system and forming the product matrix $T_E^P = E_3 E_2 E_1$, Equation (8) becomes

$$\vec{V}_P = T_E^P \vec{V}_E \tag{10}$$

Further, the choices of Euler angles were made in order to correspond with angles commonly used to describe projectile orientation throughout a trajectory. The first Euler angle, ε_1, is the azimuth component of the projectile heading relative to the initial shot line. In ballistic terminology, this is commonly called the yaw angle and is denoted by ψ. The second Euler angle, ε_2, is the elevation component of the projectile heading or, in ballisticians' parlance, the

pitch angle, θ. The third Euler angle, ε_3, is the rotation component of the projectile orientation or the roll angle, ϕ.[1]

When we perform the matrix multiplication and make the substitutions for the Euler angles, T_E^P is seen to be

$$T_E^P = \begin{pmatrix} T_1 & T_2 & T_3 \\ T_4 & T_5 & T_6 \\ T_7 & T_8 & T_9 \end{pmatrix} \tag{11}$$

in which

$$\begin{aligned} T_1 &= \cos(\theta)\cos(\psi) \\ T_2 &= \cos(\theta)\sin(\psi) \\ T_3 &= -\sin(\theta) \\ T_4 &= \sin(\theta)\sin(\phi)\cos(\psi) - \cos(\phi)\sin(\psi) \\ T_5 &= \sin(\theta)\sin(\phi)\sin(\psi) + \cos(\phi)\cos(\psi) \\ T_6 &= \cos(\theta)\sin(\phi) \\ T_7 &= \sin(\theta)\cos(\phi)\cos(\psi) + \cos(\phi)\cos(\psi) \\ T_8 &= \sin(\theta)\cos(\phi)\sin(\psi) - \sin(\phi)\cos(\psi) \\ T_9 &= \cos(\theta)\cos(\phi) \end{aligned} \tag{12}$$

The inverse transformation of a vector from projectile-fixed coordinates to earth-fixed coordinates is given by

$$\vec{V}_E = \left(T_E^P\right)^T \vec{V}_P \tag{13}$$

Equations (11) and (13) can be used to transform any vector between the earth-fixed and projectile-fixed systems. Acceleration, velocity, thrust, and line of sight are examples of vectors whose components typically are needed in both systems. Before proceeding to examples of transformations of this type of sensor data, another critical characteristic of the relationship between the earth-fixed and projectile-fixed systems needs to be considered, i.e., the projectile-fixed system is moving with respect to the earth-fixed system in both translation and orientation. The angular rates describing these orientation changes need to be formulated in each system as well.

[1]It is important to note that even though the use of ψ, θ, and ϕ to denote yaw, pitch, and roll is common in the literature, not every author defines each of these angles as is done here. Since there is no great agreement, care must be taken always by authors to rigorously define the systems they employ and by readers to understand the authors' systems.

4. Angular Rates in Projectile and Earth Systems

The angular velocity of the projectile-fixed system with respect to the earth-fixed system is described in the projectile-fixed system by a vector $\vec{\Omega}_P = \left(\omega_{X_P}, \omega_{Y_P}, \omega_{Z_P}\right)^T$ in which ω_{X_P} is the angular velocity of the $Y_P \mid Z_P$ axes about the X_P axis; ω_{Y_P} is the angular velocity of the $Z_P \mid X_P$ axes about the Y_P axis; and ω_{Z_P} is the angular velocity of the $X_P \mid Y_P$ axes about the Z_P axis. Each of these velocities is defined herein to be right-hand positive. In ballisticians' terminology, this vector is denoted by $\vec{\Omega}_P = (p, q, r)^T$.

The angular velocity vector of the projectile-fixed system with respect to the earth-fixed system is also given by the sum of the derivatives of the Euler angles ε_1, ε_2, and ε_3. However, recalling that each of these Euler angles was defined in a different coordinate system, their derivatives need to be transformed into the projectile-fixed system before corresponding components can be added. With the ballistic terminology for the Euler angles adopted in the last section, $\dot{\vec{\varepsilon}}_1 = (0, 0, \dot{\psi})^T$ in the X_1, Y_1, Z_1 coordinate system, $\dot{\vec{\varepsilon}}_2 = (0, \dot{\theta}, 0)^T$ in the X_2, Y_2, Z_2 coordinate system, and $\dot{\vec{\varepsilon}}_3 = (\dot{\phi}, 0, 0)^T$ in the X_3, Y_3, Z_3 coordinate system. Thus, $\vec{\Omega}_P$ can also be written in terms of the Euler angles as

$$\vec{\Omega}_P = E_3 E_2 \begin{pmatrix} 0 \\ 0 \\ \dot{\psi} \end{pmatrix} + E_3 \begin{pmatrix} 0 \\ \dot{\theta} \\ 0 \end{pmatrix} + \begin{pmatrix} \dot{\phi} \\ 0 \\ 0 \end{pmatrix} \tag{14}$$

Making the substitutions for E_2 and E_3 from Equations (6) and (9) and doing the algebra yields

$$\vec{\Omega}_P = \begin{pmatrix} \dot{\phi} - \dot{\psi}\sin(\theta) \\ \dot{\theta}\cos(\phi) + \dot{\psi}\cos(\theta)\sin(\phi) \\ -\dot{\theta}\sin(\phi) + \dot{\psi}\cos(\theta)\cos(\phi) \end{pmatrix}. \tag{15}$$

The relationships between the body-fixed components of projectile angular motion and the roll, pitch, and yaw rates are thus given by

$$\begin{aligned} p &= \dot{\phi} - \dot{\psi}\sin(\theta) \\ q &= \dot{\theta}\cos(\phi) + \dot{\psi}\cos(\theta)\sin(\phi) \\ r &= -\dot{\theta}\sin(\phi) + \dot{\psi}\cos(\theta)\cos(\phi) \end{aligned} \tag{16}$$

Solving for the Euler angle derivatives in terms of the projectile-fixed rates gives

$$\begin{aligned}\dot{\phi} &= p + \left[q\sin(\phi) + r\cos(\phi) \right]\tan(\theta) \\ \dot{\theta} &= q\cos(\phi) - r\sin(\phi) \\ \dot{\psi} &= \left(q\sin(\phi) + r\cos(\phi)\right)/\cos(\theta)\end{aligned} \tag{17}$$

As seen later in this report, there are commonly used, body-fixed sensor systems designed to measure p, q, and r and other systems that respond to $\dot{\phi}$, $\dot{\theta}$, and $\dot{\psi}$. Failure to appreciate the differences among these quantities can lead to erroneous interpretations of sensor data. Conversely, appreciation of these differences sometimes can provide additional insights concerning projectile dynamics.

5. Body-Fixed Sensor Locations and Orientations

The location of a sensor on a flight body can greatly affect its output. In some cases, the quantity being measured is location dependent, e.g., acceleration at a point on the body. In other cases, the sensor response is affected by something besides the primary stimulus that it is designed to measure, e.g., the gain of an angular rate sensor might be g-sensitive. In both instances, the locations and the orientations of the sensors must be known in order to correctly interpret their output in the projectile-fixed coordinate system even before a transformation into the earth-fixed navigation system. Seldom, if ever, will it be possible to install sensors at arbitrary locations on projectiles. Although greater possibilities might exist in a developmental or test configuration, tactical configurations usually have only limited space at predetermined locations available for on-board sensors and electronics. Linear accelerometers provide an illustrative example of the effects of sensor location and orientation.

The basic equation relating position (P), velocity (V), and acceleration (A) is $P(t) = P(0) + V(0)\,t + \int_0^t \int_0^t A\,\partial t$. For projectile locations along a trajectory as measured in the earth-fixed system, the vector version of this relationship is

$$\begin{pmatrix} x(t)_E \\ y(t)_E \\ z(t)_E \end{pmatrix} = \begin{pmatrix} x(0)_E \\ y(0)_E \\ z(0)_E \end{pmatrix} + \begin{pmatrix} \dot{x}(0)_E\, t \\ \dot{y}(0)_E\, t \\ \dot{z}(0)_E\, t \end{pmatrix} + \int_0^t \int_0^t \begin{pmatrix} a_{X_E} \\ a_{Y_E} \\ a_{Z_E} \end{pmatrix} \partial t \tag{18}$$

Beginning with acceleration and velocity components in the projectile-fixed coordinate system, this relationship becomes

$$\begin{pmatrix} x(t)_E \\ y(t)_E \\ z(t)_E \end{pmatrix} = \begin{pmatrix} x(0)_E \\ y(0)_E \\ z(0)_E \end{pmatrix} + \left(T_E^P\right)^T \begin{pmatrix} \dot{x}(0)_P\, t \\ \dot{y}(0)_P\, t \\ \dot{z}(0)_P\, t \end{pmatrix} + \int_0^t \int_0^t \left(T_E^P\right)^T \begin{pmatrix} a_{X_E} \\ a_{Y_E} \\ a_{Z_E} \end{pmatrix} \partial t \qquad (19)$$

In ballisticians' terminology the velocity vector in the projectile-fixed coordinate system is $\begin{pmatrix} u \\ v \\ w \end{pmatrix} = \begin{pmatrix} \dot{x}_P \\ \dot{y}_P \\ \dot{z}_P \end{pmatrix}$ and the acceleration vector is $\begin{pmatrix} \dot{u} \\ \dot{v} \\ \dot{w} \end{pmatrix}$. Thus, ballisticians rewrite Equation (19) as

$$\begin{pmatrix} x(t)_E \\ y(t)_E \\ z(t)_E \end{pmatrix} = \begin{pmatrix} x(0)_E \\ y(0)_E \\ z(0)_E \end{pmatrix} + \left(T_E^P\right)^T \begin{pmatrix} u(0)\, t \\ v(0)\, t \\ w(0)\, t \end{pmatrix} + \int_0^t \int_0^t \left(T_E^P\right)^T \begin{pmatrix} \dot{u} \\ \dot{v} \\ \dot{w} \end{pmatrix} \partial t \qquad (20)$$

Considering only the axial acceleration component, $\dot{u}$, the process required to obtain this quantity from projectile-fixed sensor data can be complicated. Designating a location on board a rigid projectile with unchanging mass properties as $\left(L_{X_P}, L_{Y_P}, L_{Z_P}\right)^T$ where each component is measured from the projectile's c.g., the ballisticians' equation for the axial acceleration at that point is given by

$$A_{X_P} = \dot{u} + qw - rv - \left(q^2 + r^2\right)L_{X_P} + \left(pq - \dot{r}\right)L_{Y_P} + \left(pr + \dot{q}\right)L_{Z_P} \qquad (21)$$

Because gravity cannot be sensed by an accelerometer on board a projectile in free flight, the idealized output $\left(S_{X_P}\right)$ of an axial accelerometer at this location is thus

$$S_{X_P} = \dot{u} + qw - rv + \left(-q^2 - r^2\right)L_{X_P} + \left(pq - \dot{r}\right)L_{Y_P} + \left(pr + \dot{q}\right)L_{Z_P} + g\sin(\theta) \qquad (22)$$

In order to simplify notation, sensed acceleration components parallel to the projectile-fixed axes are usually referred to as Acc_I (+X_P direction), Acc_J (+Y_P direction), and Acc_K (+Z_P direction). Similarly, sensor offsets are usually given as Δi, Δj, and Δk. Thus, Equation (22) is usually written as

$$Acc\_I = \dot{u} + qw - rv + \left(-q^2 - r^2\right)\Delta i + \left(pq - \dot{r}\right)\Delta j + \left(pr + \dot{q}\right)\Delta k + g\sin(\theta) \qquad (23)$$

The difference between axial acceleration ($\dot{u}$) and an idealized axial accelerometer's output (Acc_I) can be better appreciated graphically. With a six-degree-of-freedom computer model, the trajectory of an M483 artillery projectile was simulated for a launch at 25° quadrant elevation and 340-m/s muzzle velocity. Figure 7 shows the axial acceleration throughout the trajectory and Figure 8 shows the output of an ideal axial accelerometer at the projectile c.g., $L=(0,0,0)^T$. The difference between the two curves is primarily attributable to the absence of the gravity component in the sensed acceleration in Figure 8 because $|qw - rv| < 0.0003\,g$.

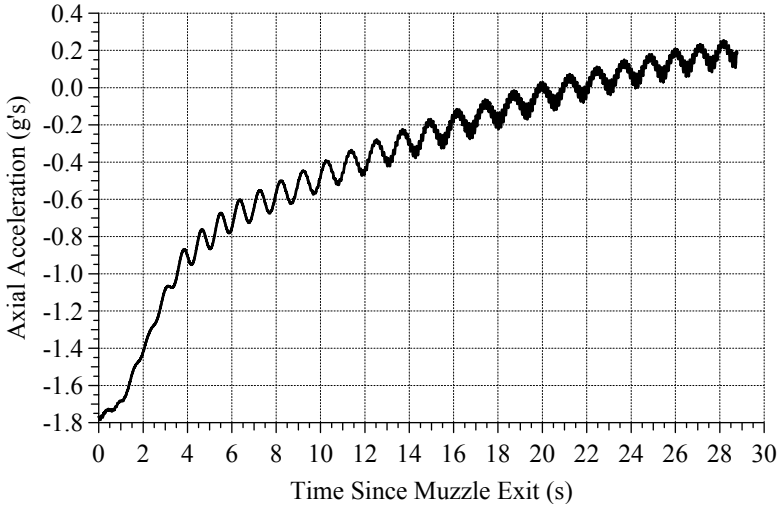

Figure 7. Axial acceleration ($\dot{u}$) for modeled M483 trajectory.

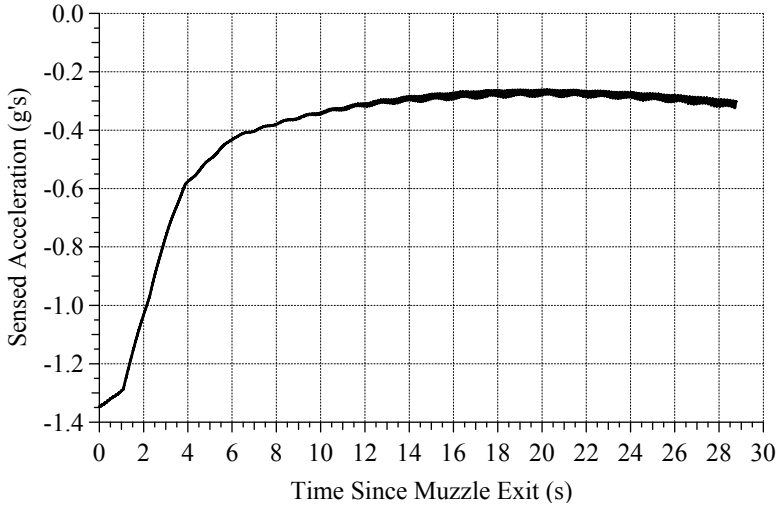

Figure 8. Sensed axial acceleration at the c.g. for modeled M483 trajectory.

When the axial accelerometer is installed in the fuze, as is typical in flight experiments, the location would be approximately 0.45 m forward of the c.g. The sensed axial acceleration at this location, $L = (0.45,0,0)^T$, is shown in Figure 9. For an accelerometer 2 mm off the projectile spin axis, e.g., $L = (0.45,0.0014,0.0014)^T$, the sensed acceleration is shown in Figure 10.

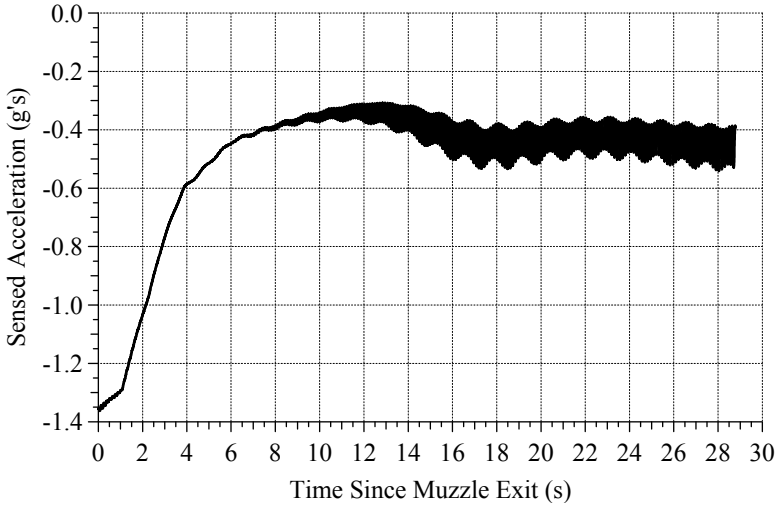

Figure 9. Sensed axial acceleration 0.45 m forward of the c.g. for modeled M483 trajectory.

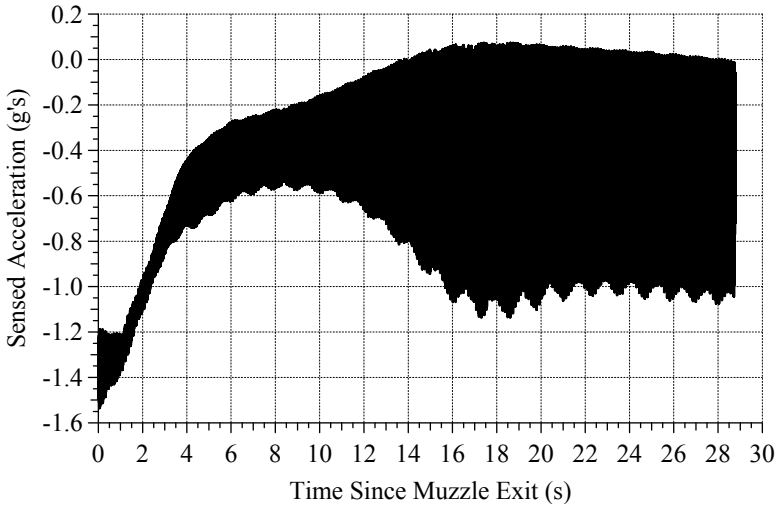

Figure 10. Sensed axial acceleration 0.45 m forward of the c.g. and 2 mm off the spin axis for modeled M483 trajectory.

Despite the lack of resemblance of the curve in Figure 10 to the curve in Figure 7, axial acceleration ($\dot{u}$) can be derived from accelerometer output, given initial conditions, knowledge of the location of an axial accelerometer, and knowledge of the angular velocity, $(p,q,r)^T$, and acceleration, $(\dot{p},\dot{q},\dot{r})^T$, of the projectile. These rates are estimated by other on-board sensors.

In the preceding examples, the accelerometers were assumed to be exactly situated at known points and to have their sensitive axes oriented exactly parallel to the projectile spin axis. Neither assumption is realizable in an actual system because of location and alignment

uncertainties arising from tolerances in the manufacturing and assembly processes. Additionally, linear accelerometers typically have some level of sensitivity to accelerations in directions other than the direction of the measurement axis. These uncertainties must be resolved in order to correctly interpret the sensor output and to derive desired quantities from the output. We can accomplish this resolution by calibrating the individual sensors either in the laboratory or in flight.

6. Sensor Locations in the Aeroballistic Diagnostic Fuze

The aeroballistic diagnostic fuze (DFuze) (U.S. Patent 6349652) was developed at ARL as a high-g, projectile-borne system for non-intrusive measurements of projectile diagnostics and aerodynamic performance. The current nominal DFuze instrumentation configuration (designated as the DF2K1 series) combines patented optical sensors, a unique constellation of accelerometers and magnetic sensors, analog and digital electronics, and telemetry components. DFuzes can and have been built to conform to individual projectile form factor requirements. The DF2K1 DFuze maintains the interface characteristics of a standard North Atlantic Treaty Organization-compatible 155-mm artillery fuze. An example is shown in the upper half of Figure 11. Two of the four solar light-indicating transducers (SLITs) (U.S. Patent 5909275) used in the solarsonde system for measuring projectile heading and projectile crossing rate with respect to the sun can be seen in this view. As the schematic in the lower half of Figure 11 shows, the radial axes of the projectile-fixed coordinate system are defined so that SLIT No. 1 is in the $+X_P|Z_P$ plane. Locations within the DFuze body of all the components are specified, and laboratory calibrations are used to better measure installed locations and orientations of the sensing elements. The locations are then transformed to the projectile-fixed system by the addition of the components of the offset of the DFuze from the projectile c.g. For rigid projectiles with unchanging mass properties, this is a fixed offset. For flexible projectiles, projectiles with components in relative motion (e.g., de-spun nose), and projectiles with changing mass properties (e.g., through fuel consumption or cargo ejection), c.g. can change in flight, and location-sensitive, projectile-fixed sensors' output will be affected.

Besides the four solarsonde SLITs, a DF2K1 DFuze contains six accelerometers, a temperature sensor, and a magnetometer mounted on an ARL-designed board. This board is indexed to the DFuze housing so that the sensor locations are duplicated in each DFuze within manufacturing and installation tolerances. Figure 12 shows the forward side of the board as installed within the DFuze with the projectile-fixed axes and identifying letters superimposed on the picture. The component labeled A is a 3-axis magnetometer with its axes nominally oriented parallel to the projectile axes and with the same parity as the projectile axes. The output of some magnetometers (and other non-inertial sensors) is affected by the inertial forces to which the magnetometers are subjected while they measure the primary stimulus. Because of this, the location parameters as well as the orientation parameters of these sensors must be known in

order to correctly interpret their output. In order to simplify notation, each magnetometer's three axes are usually referred to as Mag_I ($+X_P$ direction), Mag_J ($+Y_P$ direction), and Mag_K ($+Z_P$ direction). The component labeled "B" is a single-axis accelerometer used to measure thrust and drag. This sensor's axis is ideally situated on the projectile's X_P axis and oriented in the $+X_P$ direction and is commonly called Acc_I. The axial component (Δi) of this sensor's location is its offset from the c.g. of the assembled projectile with fuze. Component "C" is a temperature sensor, which can be used to compensate for the variations in bias and/or scale factor with temperature, which are characteristic of many sensors. The remaining unlabeled components are various supporting electronics.

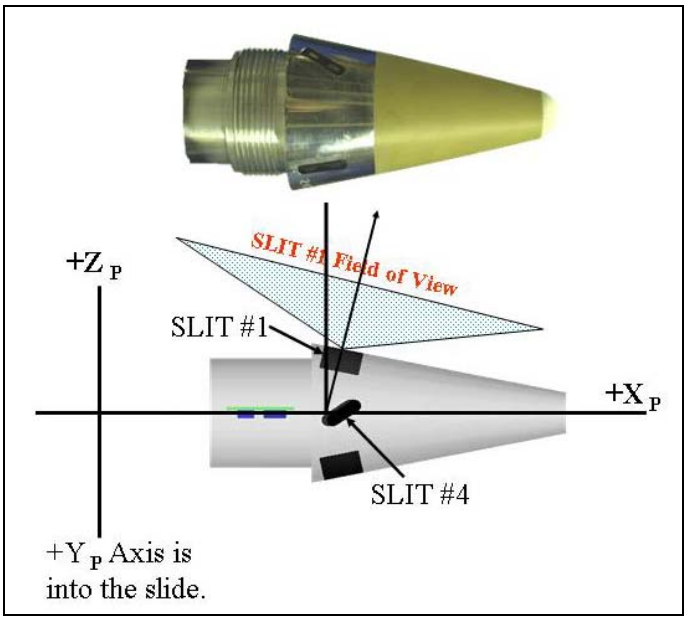

Figure 11. DF2K1 DFuze configuration.

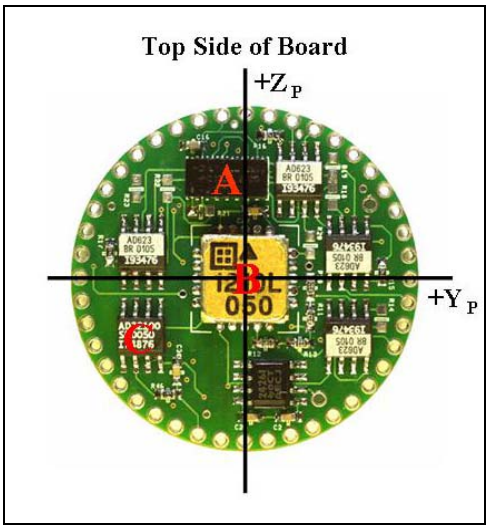

Figure 12. DF2K1 sensor board viewed from forward looking aft.

On the aft side of the board (see Figure 13), there are five accelerometers, labeled D, E, F, G, and H. Accelerometer D is a bi-axial device whose sensitive axes are ideally situated on the projectile spin axis and oriented parallel to the Y_P and Z_P axes. The axial location of accelerometer D is measured from the c.g. of the projectile with fuze assembly. These sensor axes are usually called Acc_J (-Y_P direction) and Acc_K (+Z_P direction). The orientation of the Acc_J axis in the -Y_P direction is an artifact of accelerometer D being mounted on the aft side of the sensor board. A parity correction of the Acc_J output is made during data reduction to provide acceleration measurements in the projectile-fixed coordinate system. Accelerometers E, F, G, and H are single-axis devices whose output is combined on board the projectile to provide an estimate of the projectile spin rate. This collection of sensors is called the accelerometer spin ring or the accel_ring for short. In ballisticians' notation, the equations for sensed acceleration at a point in the +Y_P and the +Z_P directions are

$$S_{Y_P} = \dot{v} + ru - pw + (pq + \dot{r})L_{X_P} + (-p^2 - r^2)L_{Y_P} + (qr - \dot{p})L_{Z_P} - g\cos(\theta)\sin(\phi) \quad (24)$$

$$S_{Z_P} = \dot{w} + pv - qu + (pr - \dot{q})L_{X_P} + (qr + \dot{p})L_{Y_P} + (-p^2 - q^2)L_{Z_P} - g\cos(\theta)\cos(\phi) \quad (25)$$

With the simplified notation of Equation (22), these equations become

$$Acc\_J = \dot{v} + ru - pw + (pq + \dot{r})\Delta i + (-p^2 - r^2)\Delta j + (qr - \dot{p})\Delta k - g\cos(\theta)\sin(\phi) \quad (26)$$

$$Acc\_K = \dot{w} + pv - qu + (pr - \dot{q})\Delta i + (qr + \dot{p})\Delta j + (-p^2 - q^2)\Delta k - g\cos(\theta)\cos(\phi) \quad (27)$$

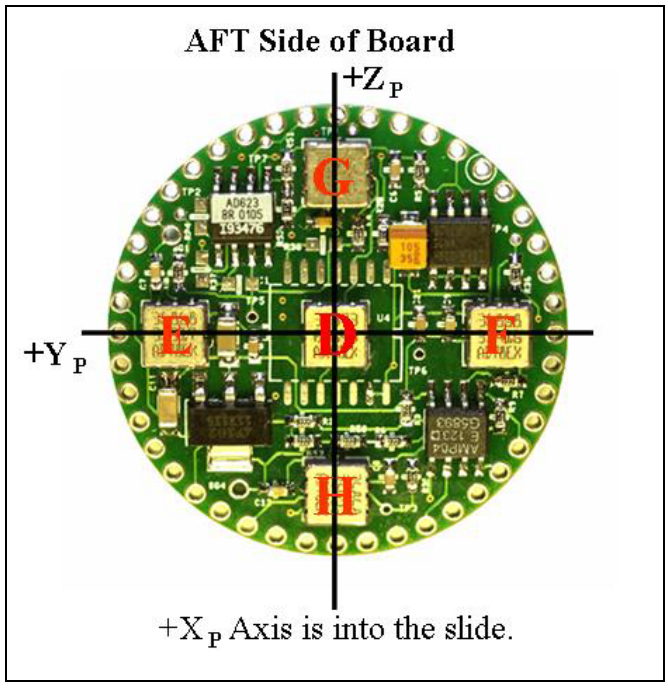

Figure 13. DF2K1 sensor board viewed from rear looking forward.

Before any flight experiment, Equations (22), (24), and (25) or alternatively, (23), (26), and (27) need to be evaluated for anticipated projectile dynamics in order to determine required accelerometer characteristics such as dynamic range and frequency response. The natures of the accelerations to which the projectile-fixed sensors will be subjected and the natures of the acceleration components in an earth-fixed or navigation coordinate system can be very different. The sensor characteristics necessary to obtain projectile-fixed measurements of sufficient accuracies to meet required earth-fixed measurement accuracies are the design performance requirements. These requirements cannot be understood without an appreciation of the relationship between a sensor's location and orientation and that sensor's stimuli.

7. Estimating Projectile Spin Rate

Spin rate is an important characteristic of any projectile's flight. This rate (p in ballisticians' notation) is defined in the projectile-fixed system as the angular velocity of the Y_P- Z_P axes about the X_P axis. The DFuze does not include any sensor that directly measures spin rate. Because of size, high-g survivability, and cost requirements and the necessity for sometimes estimating spin rates of 300 Hz and more, traditional angular rate measurement devices such as gyroscopes have not been included in the DFuze. Perhaps there will someday be micro-electro-mechanical devices suitable for inclusion in future DFuzes, but at present, spin rate estimates are made from accel_ring, solarsonde, and magnetometer measurements.

7.1 Accel_Ring Measurements

The four accelerometers in the accel_ring (see Figure 13) are installed in opposed pairs about the projectile spin axis with the sensor axes of each pair co-linear with the diameter upon which they are situated and co-directional in orientation. That is, the sensitive axes of accelerometers E, F, G, and H are oriented in the $+Y_P$, $+Y_P$, $+Z_P$, and $+Z_P$ directions, respectively. The differences between the sensed accelerations from two such pairs on the Y_P axis (F,E) and the Z_P axis (H,G) are

$$\begin{aligned} \mathrm{Acc\_J_F} - \mathrm{Acc\_J_E} &= (\Delta j_F - \Delta j_E)(-p^2 - r^2) \\ \mathrm{Acc\_K_H} - \mathrm{Acc\_K_G} &= (\Delta k_H - \Delta k_G)(-p^2 - q^2) \end{aligned} \tag{28}$$

If $|\Delta j_E| = |\Delta j_F| = |\Delta k_G| = |\Delta k_H| = R$, then

$$\mathrm{Acc\_J_F} - \mathrm{Acc\_J_E} + \mathrm{Acc\_K_H} - \mathrm{Acc\_K_G} = 4R\left(p^2 + \frac{r^2 + q^2}{2}\right) \tag{29}$$

$$\frac{\mathrm{Acc\_J_F} - \mathrm{Acc\_J_E} + \mathrm{Acc\_K_H} - \mathrm{Acc\_K_G}}{4R} = \left(p^2 + \frac{r^2 + q^2}{2}\right) \tag{30}$$

This arithmetic is done on board the DFuze, and the telemetered measurement is the quantity given by Equation (30). When $p^2 >> \frac{r^2 + q^2}{2}$, as is often the case, a good estimate of the projectile spin rate is obtained from the accel_ring output by

$$\overline{p} \approx \sqrt{\left(p^2 + \frac{r^2 + q^2}{2} \right)} \quad . \tag{31}$$

7.2 Solarsonde Measurements

The four SLIT optical sensors installed in the DF2K1 DFuze are designed to produce a significant output when aligned with the sun and almost no output when not aligned. On board a spinning projectile, these sensors provide a pulse train, which when combined with calibration data, yields a measurement of the angle between the spin axis and the vector to the sun (σ_s, called the solar aspect angle) and a solar roll history. Figure 14 shows a sample of telemetered solarsonde data from a DFuze mounted in a stationary spin fixture. The signals from all four SLITs are combined on board the projectile into a single output stream. The spikes on the graph of this combined waveform occur when the respective SLITs are aligned with the sun during a projectile rotation. The combination of gains and parities of the four SLITs are varied so that the output from each sensor can be identified (as is indicated by the numerals on the plot). Also shown are two simple period measurements that can provide a solar roll rate estimate.

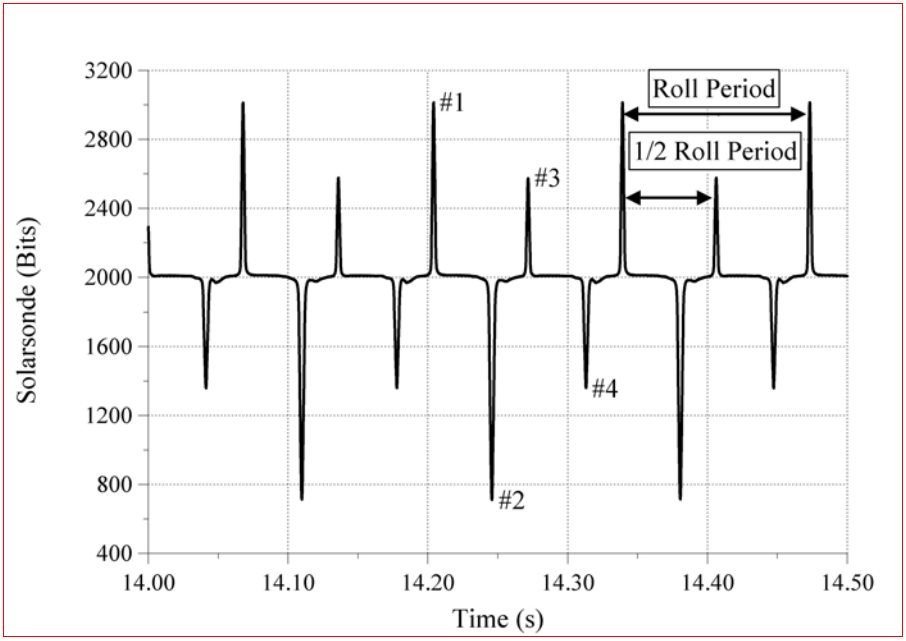

Figure 14. Sample of Solarsonde data

If a projectile's spin rate (p) or solar aspect angle (σ_S) changes within a roll cycle, error is introduced into the period-based solar roll rate estimate. In this instance, a more accurate roll rate estimate is obtained by the correlation of the solar aspect angle at each SLIT alignment with the roll angle at that alignment measured during laboratory calibration. Summation of the amount of roll required for each succeeding SLIT alignment yields an accumulated roll angle versus time history. First and second derivatives give estimates of solar roll rate and roll acceleration, respectively. These estimates are more accurate than those obtained from period measurements because of the greater frequency of roll orientation measurements. This methodology is typically employed in the processing of flight data.

7.3 Magnetometer Measurements

Figure 15 shows the data from one of the radial magnetometer axes (Mag_J) during the same time period. Period measurements between signal extrema are used to estimate projectile roll rate with respect to the magnetic field. In contrast to the SLITs in the solarsonde system, which are designed to be nearly impulsive in their responses, vector magnetometers provide continuous response where the amplitude of the output signal varies directly with the projection of the local magnetic field onto the sensor axis. With knowledge of the local magnetic field and a sensor that is accurately located, aligned, and calibrated, we can directly derive projectile heading with respect to the magnetic field from an amplitude measurement. When, as is usually the case with actual implementations, any of these assumptions is violated, advanced processing techniques are employed to remove the effects of these errors.

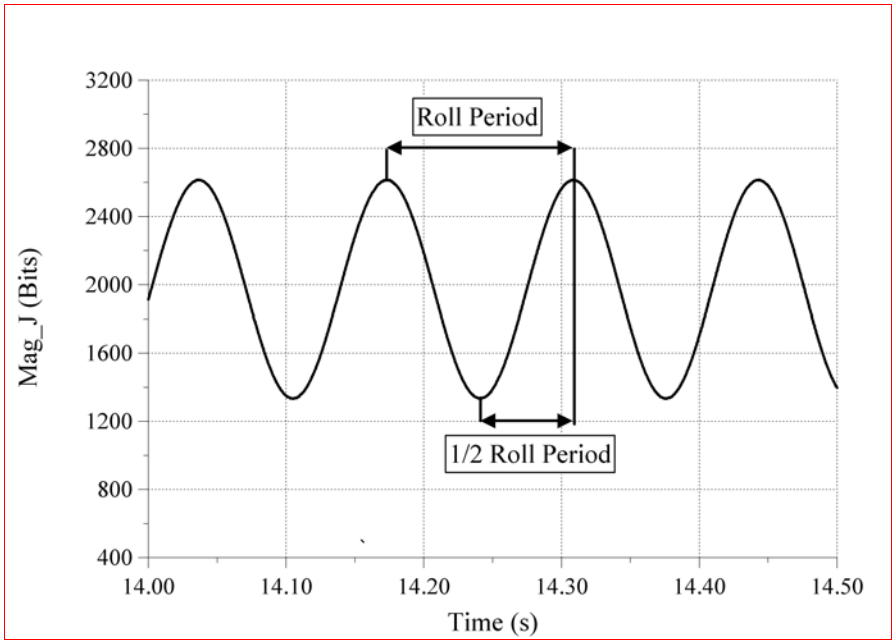

Figure 15. Sample of radial magnetometer data.

For these solar and magnetic sensor systems, what is being measured is not the projectile spin rate but the rate at which the optical and magnetic sensors are swept past the sun and the earth's magnetic field, respectively. The equations for these rates are the same as the equation for the derivative of the Eulerian roll angle (Equation [17]) with appropriate change of variables. With S and M subscripts to indicate solar and magnetic, respectively, these equations are, with the necessary changes,

$$\dot{\phi}_S = p + \left[q\sin(\phi_S) + r\cos(\phi_S) \right]\tan(\theta_S) \tag{32}$$

$$\dot{\phi}_M = p + \left[q\sin(\phi_M) + r\cos(\phi_M) \right]\tan(\theta_M) \tag{33}$$

Since solar roll rate and magnetic roll rate are entirely analogous, further discussion is restricted to solar roll rate. With some manipulation, Equation (32) becomes

$$\begin{aligned} \dot{\phi}_S &= p + \left[q\sin(\phi_S) + r\cos(\phi_S) \right]\left[\frac{\cos(\theta_S)}{\cos(\theta_S)} \right]\tan(\theta_S) \\ &= p + \left[\frac{q\sin(\phi_S) + r\cos(\phi_S)}{\cos(\theta_S)} \right]\cos(\theta_S)\tan(\theta_S) \\ &= p + \left[\dot{\psi}_S \cos(\theta_S) \right]\tan(\theta_S) \end{aligned} \tag{34}$$

With the recognition that the term $\left[\dot{\psi}_S \cos(\theta_S) \right]$ is the component of projectile yawing rate perpendicular to the plane defined by the projectile spin axis and the solar vector, that $\theta_s = 90 - \sigma_s$, and the realization that Equation (34) holds for any earth-fixed field, the relationship between projectile roll rate with respect to any such field and projectile spin rate can be stated thus. Roll rate is the sum of spin rate and the product of the out-of-plane yawing rate and the tangent of the complement of the angle between the spin axis and the field vector. Roll rate and spin rate are equal when there is no yawing motion $\left(\dot{\psi} = 0\right)$ or the spin axis is perpendicular to the field vector $\left(\sigma = 90, \therefore \theta = 0\right)$ and unequal when $\dot{\psi} \neq 0$ and $\sigma \neq 90$. This relationship and the relationship between spin rate and accel_ring data have sometimes provided crucial insight into projectile dynamics not attainable from other measurements.

8. Summary

Body-fixed sensors combined with a telemetry system provide measurements of projectile in-flight dynamics not achievable with stationary or remote sensing systems such as radar or cameras. Body-fixed sensor systems on board the projectiles provide continuous data throughout a flight, but many of the desired performance metrics are defined in an earth-fixed coordinate system. It is therefore crucial that the relationship between these two systems be understood for

the proper design of projectile-fixed sensor systems and for the correct interpretation of sensor data obtained during flight experiments.

The mathematics describing this relationship have been presented herein and examples have been provided for the sensor systems included within the DFuze measurement system, i.e., accelerometers, vector magnetometers, and solarsondes. Because these mathematics hold for any vector definable in these coordinate systems, this work is applicable to any sensor system measuring vector quantities, e.g., angular rate sensors, velocimeters, gimbaled seekers, etc.

9. Reference

1. Murphy, C.H. *Free Flight Motion of Symmetric Missiles*; BRL-1216; Ballistics Research Laboratory: Aberdeen Proving Ground, MD, July 1963.

Appendix A. Plane-Fixed Coordinate System

The basic force and moment equations from which the free flight equations of motion of a rigid projectile are derived are simplified when formulated in a non-rolling coordinate system with the same X axis as the projectile-fixed system. The plane-fixed coordinate system is such a non-rolling system with the added stipulation that the plane-fixed Y axis is in the horizontal plane. Thus, the plane-fixed Z axis is in the vertical plane containing the spin (X) axis. Designating the axes with an FP subscript, the plane-fixed system is shown in Figure A-1.

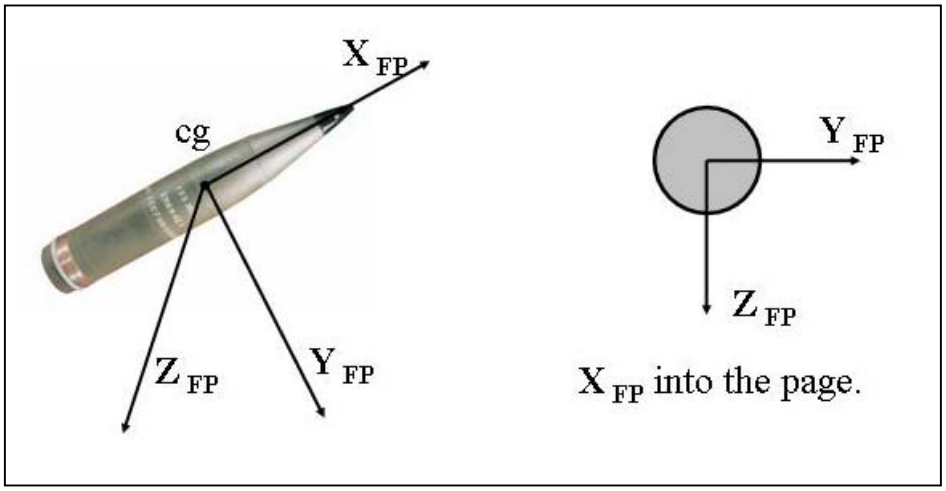

Figure A-1. Plane-fixed coordinate system.

The plane-fixed system is used extensively in computer trajectory simulations since the differential equations of motion can be evaluated at larger integration time steps in this coordinate system than in the projectile-fixed system. The plane-fixed system already was seen in Section 3 of this report although it was not so named at that time. The X_2, Y_2, Z_2 system that resulted from the second Euler rotation is the plane-fixed system. The transformation matrix from earth- to plane-fixed vectors, given by substituting the Euler angles and evaluating the matrix multiplication in Equation (5), is

$$T_E^{FP} = \begin{pmatrix} \cos(\theta)\cos(\psi) & \cos(\theta)\sin(\psi) & -\sin(\theta) \\ -\sin(\psi) & \cos(\psi) & 0 \\ \sin(\theta)\cos(\psi) & \sin(\theta)\sin(\psi) & \cos(\theta) \end{pmatrix} \tag{A-1}$$

The transformation matrix from the plane-fixed to the projectile-fixed system has already been given in Equation (9). Substituting the Euler roll angle, this becomes

$$T_{FP}^{P} = \begin{pmatrix} 0 & 0 & 1 \\ 0 & \cos(\phi) & \sin(\phi) \\ 0 & -\sin(\phi) & \cos(\phi) \end{pmatrix} \tag{A-2}$$

NO. OF COPIES ORGANIZATION

1 ADMINISTRATOR
DEFENSE TECHNICAL INFO CTR
ATTN DTIC OCA
8725 JOHN J KINGMAN RD STE 0944
FT BELVOIR VA 22060-6218

1 DIRECTOR
US ARMY RSCH LABORATORY
ATTN AMSRL CI IS R REC MGMT
2800 POWDER MILL RD
ADELPHI MD 20783-1197

1 DIRECTOR
US ARMY RSCH LABORATORY
ATTN AMSRL CI OK TECH LIB
2800 POWDER MILL RD
ADELPHI MD 20783-1197

1 DIRECTOR
US ARMY RSCH LABORATORY
ATTN AMSRL D D SMITH
2800 POWDER MILL RD
ADELPHI MD 20783-1197

5 DIR US ARMY RSCH LABORATORY
ATTN AMSRL SE S J EIKE
AMSRL SE SA J PRICE
AMSRL SE SS LADAS
A EDELSTEIN D FLIPPEN
2800 POWDER MILL RD
ADELPHI MD 20783-1197

1 DIRECTOR
US ARMY RESEARCH LABORATORY
ATTN AMSRL WM MB A FRYDMAN
2800 POWDER MILL RD
ADELPHI MD 20783-1197

1 US ARMY CECOM RDEC
ATTN AMSEL RD C2 CS J VIG
FORT MONMOUTH NJ 07703-5601

3 CDR US ARMY TACOM ARDEC
ATTN AMSTA AR FSF T S CHUNG
W TOLEDO
T RECCHIA
PICATINNY ARSENAL NJ 07806-5000

4 CDR US ARMY TACOM ARDEC
ATTN AMSTA AR FSP S PEARCY
AMSTA AR FSP M HOLLIS
P GRANGER D CARLUCCI
PICATINNY ARSENAL NJ 07806-5000

NO. OF COPIES ORGANIZATION

2 CDR US ARMY TACOM ARDEC
ATTN AMSTA AR FS A WARNASCH
AMSTA AR FSA K CHIEFA
PICATINNY ARSENAL NJ 07806-5000

1 CDR US ARMY TACOM ARDEC
ATTN AMSTA AR RMP N GRAY
PICATINNY ARSENAL NJ 07806-5000

1 CDR US ARMY TACOM ARDEC
ATTN SFAE GCSS ARMS C GRASSANO
PICATINNY ARSENAL NJ 07806-5000

1 CDR US ARMY TACOM ARDEC
DEV PROJ OFFICER (DPO) CCF
ATTN ROBERT WERKO
BLDG 94
PICATINNY ARSENAL NJ 07806-5000

1 DARPA/MTO
ATTN C NGUYEN
3701 N FAIRFAX DRIVE
ARLINGTON VA 22203-1714

7 CDR NAVAL SURF WARFARE CTR
ATTN G33 J FRAYSSE G32 ELLIS
G34 H WENDT M HAMILTON
G61 LARACH D HAGEN M M KELLY
17320 DAHLGREN ROAD
DAHLGREN VA 22448-5100

1 CDR NAWC WEAPONS DIV
ATTN G BORGEN
CODE 543200E BLDG 311
POINT MUGU CA 93042-5000

3 CDR NAVAL AIR WARFARE CTR
WEAPONS DIVISION
ATTN CODE C3923 S GATTIS
CODE C3904 D SCOFIELD
S MEYERS
CHINA LAKE CA 93555-6100

4 PROGRAM MANAGER ITTS PEO STRI
ATTN AMFTI EL D SCHNEIDER
R COLANGELO R CARPENTER
C GOODWIN
12350 RESEARCH PKWY
ORLANDO FL 32826-3276

1 DIRECTOR
US ARMY RTTC
ATTN STERT TE F TD R EPPS
REDSTONE ARSENAL AL 35898-8052

NO. OF COPIES ORGANIZATION

3 CDR US ARMY AMCOM
ATTN AMSAM RD MG NC P RUFFIN
V LEFEVRE
AMSAM RD WS DP TD C ROBERTS
REDSTONE ARSENAL AL 35898-5247

1 TEST ARTICLE PREP DEP
NAWCAD CODE 540000A
R FAULSTICH
BLDG 1492 UNIT 1
PATUXENT MD 20670-1456

1 ARROW TECH ASSOCIATES
ATTN W HATHAWAY
1233 SHELBURNE RD STE 8
SOUTH BURLINGTON VT 05403

3 ATK MISSILE SYSTEMS CO
ATTN B LINDBLOM M ROBERTS
A GAUZENS
PO BOX 4648
CLEARWATER FL 33758-4648

3 ATK MISSILE SYSTEMS CO
ATTN S OWENS J PARRILL W NYGA
MAIL STOP WV0108
ALLEGHENY BALLISTICS GROUP
210 STATE ROUTE 956
ROCKET CENTER WV 26726-3548

2 ALLIANT TECHSYSTEMS
ATTN C CANDLAND R DOHRN
5050 LINCOLN DR
MINNEAPOLIS MN 55436-1097

1 SAIC
ATTN D HALL
1100 FIRST AVE STE 300
KING OF PRUSSIA PA 19406

1 SAIC
ATTN M PALMER
1410 SPRING HILL RD STE 400
MCLEAN VA 22102

1 SAIC
ATTN JIM NORTHRUP
8500 NORMANDALE LAKE BLVD
SUITE 1610
BLOOMINGTON MN 55437

1 MACROVISION
ATTN T MACDONALD
120 EASTWAY
READING MA 01867

NO. OF COPIES ORGANIZATION

1 SWALES AEROSPACE
ATTN Q LAM
5050 POWDER MILL RD
BELTSVILLE MD 20705

1 JOHNS HOPKINS UNIV
APPLIED PHYSICS LABORATORY
ATTN W D'AMICO
1110 JOHNS HOPKINS RD
LAUREL MD 20723-6099

5 CHLS STARK DRAPER LAB
ATTN J SITOMER T EASTERLY
R POLUTCHKO F HARRISON
A KOUREPENIS
555 TECHNOLOGY SQUARE
CAMBRIDGE MA 02139-3563

2 ANALOG DEVICES
ATTN B SULOFF S LEWIS
21 OSBORN ST
CAMBRIDGE MA 02139-3556

1 ANALOG DEVICES
ATTN R MEISENHELDER
804 WOBURN ST
WILMINGTON MA 01887-3462

1 HONEYWELL
ATTN MN14-3B35 M CARUSO
12001 STATE HIGHWAY 55
PLYMOUTH MN 55441

1 SILICON DESIGNS
ATTN J COLE
1445 NW MALL ST
ISSAQUAH WA 98027

1 RAYTHEON
ATTN RON KREBS
BLDG M11 M/S 10
PO BOX 11337
TUCSON AZ 85734-1337

ABERDEEN PROVING GROUND

2 DIRECTOR
US ARMY RSCH LABORATORY
ATTN AMSRL CI OK (TECH LIB)
BLDG 305 APG AA

2 DIR USARL
ATTN AMSRL WM T ROSENBERGER
AMSRL WM B A HORST
BLDG 4600

NO. OF
COPIES ORGANIZATION

16 DIR USARL
ATTN AMSRL WM BA D LYON
J CONDON B DAVIS
T HARKINS (5) D HEPNER
G KATULKA V LEITZKE
P MULLER P PEREGINO
A THOMPSON T BROWN
M WILSON
BLDG 4600

2 DIR USARL
ATTN AMSRL WM BC P PLOSTINS
B GUIDOS
BLDG 390

1 DIR USARL
AMSRL WM BF S WILKERSON
BLDG 390

2 DIR USARL
AMSRL WM RP C SHOEMAKER
J BORNSTEIN
BLDG 1121

1 DIR USARL
ATTN AMSRL WM MB C HOPPEL
BLDG 4600

2 DIR USARL
ATTN AMSRL WM T B BURNS
AMSRL WM TC R COATES
BLDG 309

2 CDR US ARMAMENT RD&E CTR
ATTN AMSTA AR FST T R LIESKE
F MIRABELLE
BLDG 120

1 CMDR USA DTC
ATTN CSTE DTC TTM J SCHNELL
RYAN BLDG

2 CDR ATC
ATTN K MCMULLEN
G MATRICCIANI
BLDG 359